Available online at www.sciencedirect.com
ScienceDirect
Journal of Power Sources 159 (2006) 802–809
JOURNAL OF POWER SOURCES
www.elsevier.com/locate/jpowsour

Electroreduction of oxygen at polyoxometallate-modified glassy carbon-supported Pt nanoparticles

Renata Wlodarczyk [a,c], Malgorzata Chojak [b], Krzysztof Miecznikowski [b], Aneta Kolary [a,b], Pawel J. Kulesza [b,**], Roberto Marassi [a,*]

[a] *Department of Chemistry, University of Camerino, S. Agostino 1, I-62032 Camerino, Italy*
[b] *Department of Chemistry, University of Warsaw, Pasteura 1, PL-02-093 Warsaw, Poland*
[c] *Division of Chemistry, Department of Materials and Process Engineering and Applied Physics, Czestochowa University of Technology, Al. Armii Krajowej 16, PL 42-200 Czestochowa, Poland*

Received 12 September 2005; received in revised form 8 November 2005; accepted 9 November 2005
Available online 27 December 2005

Abstract

Platinum nanoparticles of ca. 8 nm diameter (that had been first deposited on glassy carbon) were subsequently modified with ultra-thin films of polyoxometallates through their spontaneous adsorption on solid (platinum and carbon) surfaces. The following polyoxometallates (Keggin type heteropolyacids), $H_3SiW_{12}O_{40}$, $H_3SiMo_{12}O_{40}$, $H_3PW_{12}O_{40}$ and $H_3PMo_{12}O_{40}$, were considered as potential activating agents.

Rotating disk voltammetry was used to probe the electroreduction of dioxygen in 0.5 mol dm^{-3} H_2SO_4 at 25 °C. For the same loading and the approximately identical distribution of platinum nanoparticles on glassy carbon, the statistically higher (in comparison to bare Pt) electrocatalytic currents for the oxygen reduction were observed upon introduction of monolayers of heteropolyanions. Out of polyoxometallates considered, the system modified with heteropolytungstate ($H_3PW_{12}O_{40}$) seemed to be the most effective in electrocatalysis. Although the possibility of structural changes cannot be excluded, the synergistic effect originated presumably from the bifunctional activity of the electrocatalyst. While Pt retained its usual reactivity towards the oxygen reduction, $H_3PW_{12}O_{40}$ could act as both effective mediator (e.g. for the reduction of the hydrogen peroxide intermediate) and the source of mobile protons at the electrocatalytic interface.

Keywords: Platinum nanoparticles; Heteropolytungstates; Heteropolymolybdates; Oxygen reduction; Electrocatalysis; Synergistic effect

1. Introduction

Since their discovery in the 19th century [1], polyoxometallates (POMs) have been exploited in many diverse areas including analytical chemistry, medicinal chemistry and catalysis, particularly in photocatalysis [1,2]. Among POMs, heteropolyacids (HPAs) of molybdenum and tungsten have been demonstrated to form thin robust electroactive films on solid (carbon, metallic or semiconductor) surfaces [3–5]. Most of modified electrodes have been fabricated using Keggin type POMs of molybdenum and tungsten [6–8]. They undergo well-defined reversible multi-electron redox transitions involving typically up to four electrons per heteropolymetallate unit. Thus, they can serve as charge relays [1,2] as well as highly effective catalysts [9] of importance to industrial catalysis [10]. In this context, HPAs exhibit Brönsted acidic properties close to the super acid region. They act as efficient oxidants, and they are characterized by very high solubility in polar solvents as well as by fairly high thermal stability in solid state.

The ability of POMs to exhibit fast reversible multi-electron transfers prompted interest in the systems as electrocatalysts for various inert redox reactions including hydrogen evolution and oxygen reduction [11–16]. It has been recognized that the partially reduced heteropolyanions of W and Mo (heteropoly-blues) provide highly reactive mixed-valence redox centers. In principle, heteropolytungstates and molybdates can be used in electrocatalysis as homogeneously dissolved species or, preferably, as materials persistently attached to electrode surfaces [12–14]. Different approaches to immobilization of POMs on electrode surfaces have been proposed. They include elec-

* Corresponding author. Tel.: +39 0737 402214; fax: +39 0737 402296.
** Corresponding author.
E-mail addresses: pkulesza@chem.uw.edu.pl (P.J. Kulesza), roberto.marassi@unicam.it (R. Marassi).

0378-7753/$ – see front matter © 2005 Elsevier B.V. All rights reserved.
doi:10.1016/j.jpowsour.2005.11.061

trodeposition [15,16], controlled fabrication of multi-layered structures by alternate immersions in the appropriate solutions of heteropolyanion and cationic (organic or inorganic) species [17], immobilization in conductive polymer matrices [18] or ion exchange polymer films [19], as well as simple attachment by adsorption on the activated carbon substrates [20].

POMs were considered for fuel cell research due to their exceptionally high solid-state protonic conductivity [21,22]. For example, hydrogen was electrocatalytically generated from steam using a sheet of polycrystalline $H_3PMo_{12}O_{40}\cdot 30H_2O$ as a conductive solid separator covered on both sides with a Pt black catalyst [23]. A low-temperature fuel cell based on a liquid phosphotungstic acid was also proposed [24,25]. A proton exchange membrane [26] was fabricated by doping the sulfonate polysulfone polymer with $H_3PW_{12}O_{40}$ (from DMF). Electrolytes composed of various POMs including $VOSO_4/H_5PMo_{10}V_2O_{40}$ or $H_3PMo_{12}O_{40}$ (cathode compartment) and $H_3PW_{12}O_{40}$ or $H_3PMo_{12}O_{40}$ (anode compartment) were also investigated [27]. The catalyst exposed to the polyoxometallate aqueous solution was found to be more tolerant to the presence of CO in hydrogen fuel [28].

Efficient electrocatalytic systems for oxygen reduction or hydrogen oxidation, in which loading of the noble metal catalyst is reduced, would utilize highly dispersed large-surface area nanosized-Pt crystallites [29–31]. In the present work, immobilization of small amounts of spherical Pt nanoparticles on the inert glassy carbon substrate is followed by modification of their surfaces with ultra-thin films of Keggin type heteropolyacids of molybdenum or tungsten. Our goal has been to combine the powerful electrocatalytic properties of platinum [32–34] with the fast electron transfer capabilities, proton mobility and high reductive reactivity of POMs [1]: $SiW_{12}O_{40}^{3-}$ (SiW_{12}), $SiMo_{12}O_{40}^{3-}$ ($SiMo_{12}$) $PW_{12}O_{40}^{3-}$ (PW_{12}) or $PMo_{12}O_{40}^{3-}$ (PMo_{12}). By analogy to parent tungsten oxides [35,36], the related polytungstates are expected to interact strongly with platinum particles and to enhance their electrocatalytic reactivity towards the reduction of oxygen [6] and the oxidation of methanol [37]. To prepare ultra-thin films of nanostructured POMs, we have explored the fact that heteropolyanions tend undergo strong adsorption on platinum and carbon substrates [38]. In particular, Pt nanoparticles can be stabilized by modifying their surfaces with robust anionic polyoxometallate monolayers [39]. The adsorptive interactions are strong enough to permit formation of stable colloidal solutions of polyoxometallate-protected Pt-nanoparticles [38,39] or carbon nanostructures [40] and related network films with two-dimensional conducting polymer interlayers. This work parallels our recent attempts to produce heteropolytungstate supported bifunctional electrocatalytic interfaces exhibiting high reactivity towards the oxidation of methanol [37].

2. Experimental

2.1. Chemicals and materials

All chemicals were commercial materials of analytical grade purity and were used without further purification. Platinum black clusters (surface area, 20 $m^2\,g^{-1}$) were obtained from Johnson and Matthew. Solutions were prepared using doubly distilled and subsequently de-ionized (Millipore Milli-Q) water. To produce a suspension of platinum nanoparticles (of ca. 8 nm diameter, as determined using transmission electron microscopy [39]), a known amount (0.1 g) of platinum black dispersed in 8 cm^3 of water was used. The suspension was sonicated for ca. 48 h. Glassy carbon (GC) disk (geometric surface area, 0.071 cm^2) served as a working electrode. Argon was used to de-aerate solutions and to keep air-free atmosphere over the solution during the measurements. All experiments were performed at room temperature (25 °C).

2.2. Electrode preparation

Before modification, glassy carbon disks were activated by polishing with successively finer grade aqueous alumina slurries (grain size, 5–0.5 μm) on a Buehler polishing cloth. To immobilize Pt nanoparticles on glassy carbon, 1 μdm^3 aliquot of Pt suspension was placed on its surface with the use of micropipette and left 15 min to dry at room temperature. To assure homogeneous and firm attachment, the electrode was placed in an oven at 60 °C for 1 h. Afterwards, the electrode was dipped into 3 mmol dm^{-3} solution of a selected polyoxometallate (POM), $H_4SiW_{12}O_{40}$ (SiW_{12}), $H_4SiMo_{12}O_{40}$ ($SiMo_{12}$), $H_3PW_{12}O_{40}$ (PW_{12}) or $H_3PMo_{12}O_{40}$ (PMo_{12}), in water for 15 min. Previous TEM results [37,39] have demonstrated by adsorption of POMs on Pt nanoparticles does not change significantly the size of the original material.

In order to verify the adsorption properties of GC and polycrystalline Pt, parallel experiments were performed using GC (diameter, 3 mm) and Pt (diameter, 2 mm) disk electrodes. Modification of the electrode surfaces with monolayer type adsorbates of the different POM were performed by dipping the electrodes for 8 h in the respective 5 mmol dm^{-3} solutions.

2.3. Electrochemical measurements

Electrochemical measurements were done with CH Instruments (Austin, U.S.A.) Model 650 workstation. Solutions were saturated with oxygen produced using a PEM electrolyzer from Quintek (Germany). A standard three-electrode cell was used for all experiments. The rotating disk voltammetric measurements were done using the Metrohom rotating disk electrode assembly. A platinum flag was used as the counter electrode. A saturated calomel electrode (SCE) was used as a reference electrode; it was placed in the second compartment and connected to the main cell through a Lugging capillary. All potentials are expressed against the reversible hydrogen electrode (RHE).

3. Results and discussion

3.1. Voltammetric identity of POMs

Our preliminary voltammetric experiments (Figs. 1–3) were aimed at providing general information about the nature of redox reactions of four Keggin type heteropolyacids of tungsten

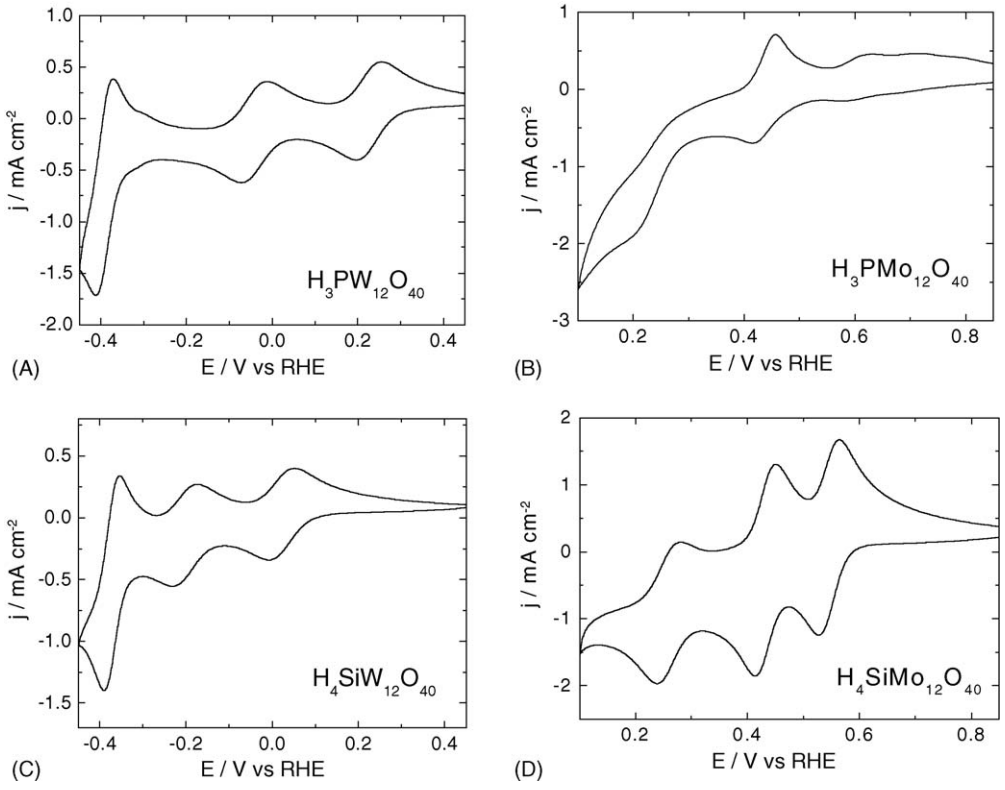

Fig. 1. Cyclic voltammetric responses of 5 mmol dm^{-3} solutions of (A) $H_3PW_{12}O_{40}$ (PW_{12}), (B) $H_3PMo_{12}O_{40}$ (PMo_{12}), (C) $H_4SiW_{12}O_{40}$ (SiW_{12}) and (D) $H_4SiMo_{12}O_{40}$ ($SiMo_{12}$) recorded at glassy carbon in 0.5 mol dm^{-3} H_2SO_4. Scan rate: 50 mV s^{-1}.

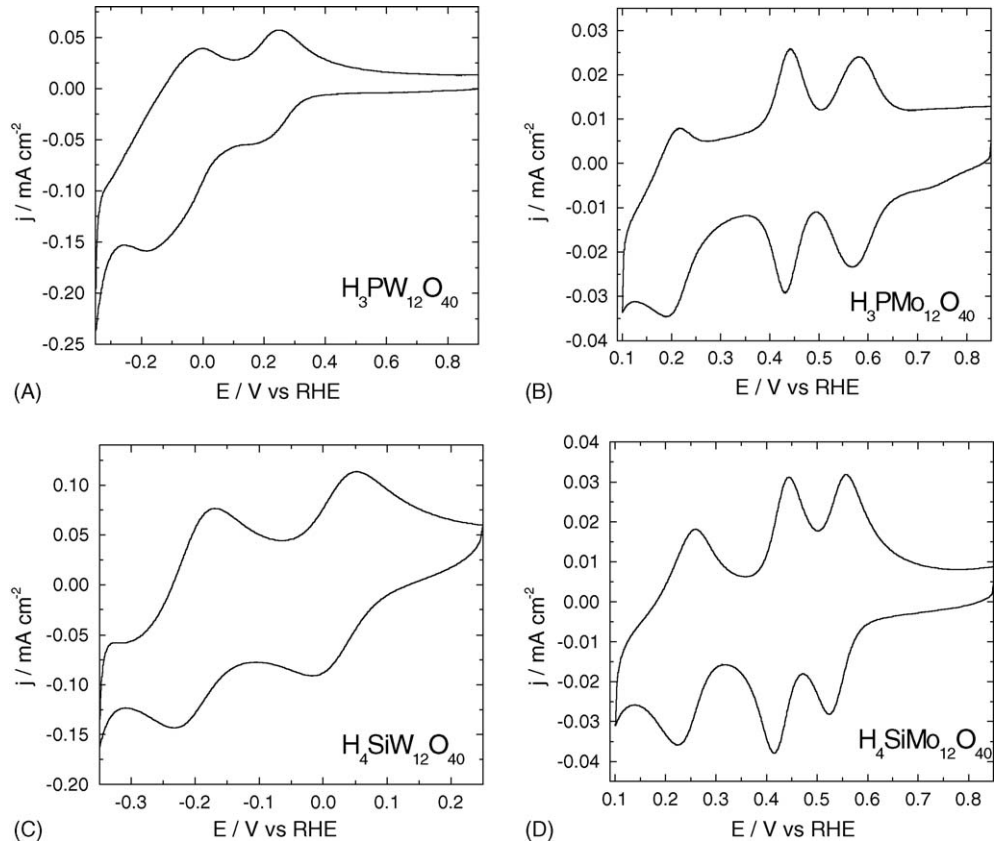

Fig. 2. Cyclic voltammetric responses of monolayer type adsorbates of (A) PW_{12}, (B) PMo_{12}, (C) SiW_{12} and (D) $SiMo_{12}$ on glassy carbon (diameter, 3 mm) recorded in 0.5 mol dm^{-3} H_2SO_4. Scan rate: 50 mV s^{-1}.

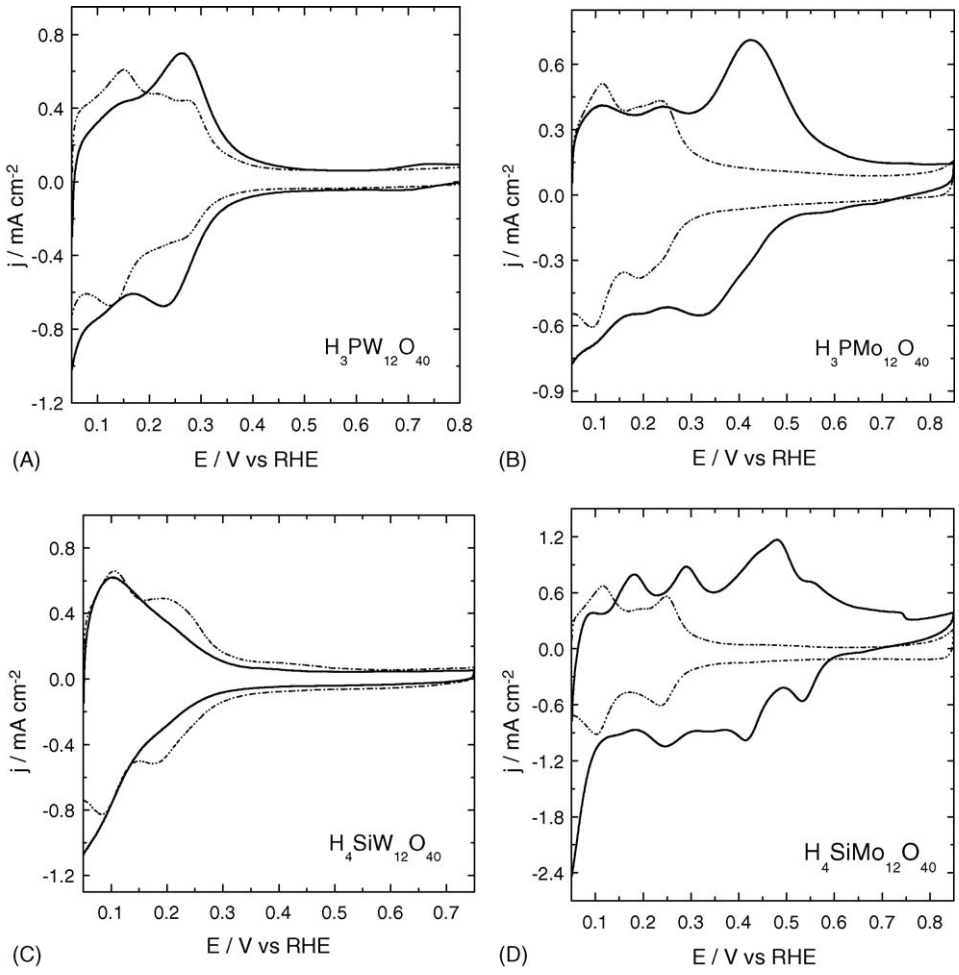

Fig. 3. Cyclic voltammetric responses of monolayer type adsorbates of (A) PW_{12}, (B) PMo_{12}, (C) SiW_{12} and (D) $SiMo_{12}$ on platinum (diameter, 2 mm) recorded in 0.5 mol dm^{-3} H_2SO_4 (deoxygenated). Scan rate: 50 mV s^{-1}. Dotted lines stand for background currents of bare Pt substrates in deoxygenated electrolytes.

and molybdenum: (A) $H_3PW_{12}O_{40}$ (PW_{12}), (B) $H_3PMo_{12}O_{40}$ (PMo_{12}), (C) $H_4SiW_{12}O_{40}$ (SiW_{12}) and (D) $H_4SiMo_{12}O_{40}$ ($SiMo_{12}$) investigated in solution and after adsorption on carbon and platinum electrode surfaces. Fig. 1 shows typical cyclic voltammetric responses of these systems dissolved in 0.5 mol dm^{-3} H_2SO_4 at 3 mmol level. It is noteworthy that electrochemical properties the POMs are characterized by multi-step electron transfers. Despite the fact that interpretation of the redox processes of PMo_{12} is more complex [41], the reactions of polymolybdate systems (curves B and D) appear at approximately 300–500 mV more positive potentials than those of the analogous polytungstates (curves A and C). The actual formal potentials also reflect the choice of heterogroup: the presence of phosphate, rather than silicate, tetrahedral unit within the tetragonal Keggin type structure tends to shift redox reactions towards more positive values.

Despite some mechanistic differences regarding the actual involvement of proton, the first two, most positive, redox reactions of Keggin type polytungstates (Fig. 1A and C) can be described in terms of two consecutive reversible one-electron processes [17]:

$$PW_{12}{}^{VI}O_{40}{}^{3-} + ne^- + nH^+ \Leftrightarrow H_nPW_n{}^{V}W_{12-n}{}^{VI}O_{40}{}^{3-} \quad (1a)$$

where n is equal to 1 or 2. The analogous reaction applies to $SiW_{12}{}^{VI}O_{40}{}^{4-}$. The third process appearing at the most negative potentials in Fig. 1A and C is two-electron in nature. In the case polymolybdates (curves B and D in Figs. 1 and 2), the three consecutive redox processes involve effectively two-electrons [41]:

$$PMo_{12}{}^{VI}O_{40}{}^{3-} + ne^- + nH^+ \Leftrightarrow H_nPMo_n{}^{V}Mo_{12-n}{}^{VI}O_{40}{}^{3-} \quad (1b)$$

where n is equal to 2, 4 or 6. The analogous reaction is expected for $SiMo_{12}{}^{VI}O_{40}{}^{4-}$. Origin of the distortion observed in the voltammetric response of Fig. 1B is unclear; but it may reflect the complexity (e.g. sensitivity to concentration or scan rate) of the voltammetric behavior of PMo_{12} [41].

Another important issue is that heteropolytungstates and heteropolymolybdates undergo irreversible adsorption (or chemisorption) on both carbon and platinum. Figs. 2 and 3 illustrate cyclic voltammograms of (A) PW_{12}, (B) PMo_{12}, (C) SiW_{12} and (D) $SiMo_{12}$ POMs adsorbed on glassy carbon (GC) and platinum electrodes, respectively, recorded in 0.5 mol dm^{-3} H_2SO_4. For PMo_{12} and PW_{12}, the monolayer type coverages on both GC and Pt have been postulated [17,38,39]. Due to the appearance

of hydrogen adsorption peaks, the existence of surface reactions related to the formation of PtO and the possibility of interference from proton reduction, the polyoxometallate responses are generally better defined when the systems are immobilized on GC (Fig. 2) rather than Pt substrates (Fig. 3). In the case of hydrogen adsorption on Pt, the overlapping effect is particularly pronounced for polytungstates (Fig. 3A and C) where hydrogen spillover has been postulated [38,39].

It is commonly accepted that, during reductions, introduction of more than four to six electrons per heteropolyunit leads to structural reorganization and irreversible redox behavior. It is apparent from Fig. 2 that, when immobilized on GC, the latter phenomena appear at potentials more negative than −0.3 and 0.1 V in the case of heteropolytungstates and heteropolymolybdates, respectively. For Pt surfaces, the practical potential limits are from ca. 1.0 to 0.1 V. Thus one can conclude that, in the potential range of interest to the voltammetric (including RDE) investigations of oxygen reduction, all POM adsorbates shall remain stable on Pt and carbon surfaces. It can be expected that they should retain electroactivity following adsorption on GC and Pt nanoparticles [38,39].

For all POM adsorbates studied (Figs. 2 and 3), the voltammetric peak currents are proportional to scan rate up to ca. 5 V s^{-1}; such characteristics are indicating a surface type behavior, and they are consistent with fast dynamic of charge transport (transfer of electrons) and charge compensating protons. Our present and previous results [17,38,39] imply rigid character of the POM attachment to Pt and GC surfaces. It is reasonable to expect that Keggin type POMs undergo similar adsorption at monolayer level on nanosized Pt (platinum black). To keep Pt on the same loading level (24 μg cm^{-2}), we have modified GC electrodes by first attaching Pt nanoparticles. To produce bifunctional electrocatalysts, the latter step has been followed by irreversible adsorption of POMs on nanostructured Pt and GC substrate.

3.2. Electrocatalysis at POM-modified carbon-supported Pt nanoparticles

To evaluate electrocatalytic activity towards the oxygen reduction of the carbon supported Pt nanoparticles modified with four different POMs (as described above), we performed the diagnostic rotating disk electrode (RDE) voltammetric measurements. Typical well-defined RDE current–potential curves recorded at 1660 rpm rotation rate in the oxygen saturated (O_2 concentration, ca. 1.1 mmol dm^{-3} [42]) 0.5 mol dm^{-3} H_2SO_4 solution are illustrated in Fig. 4 for GC supported Pt nanoparticles modified with PW_{12}, PMo_{12}, SiW_{12}, and $SiMo_{12}$. For comparison, a representative current–potential curves for the electroreduction of oxygen at GC-supported bare Pt nanoparticles is also provided. It is noteworthy that for all systems studied (Fig. 4), the loading, distribution and morphology of carbon supported Pt nanoparticles were approximately the same. Indeed, we started from the preparation of the same glassy carbon supported Pt nanoparticles, i.e. prepared using the same procedure and yielding approximately the same (within 5%) the oxygen reduction RDE voltammetric currents (Fig. 4); such platinized

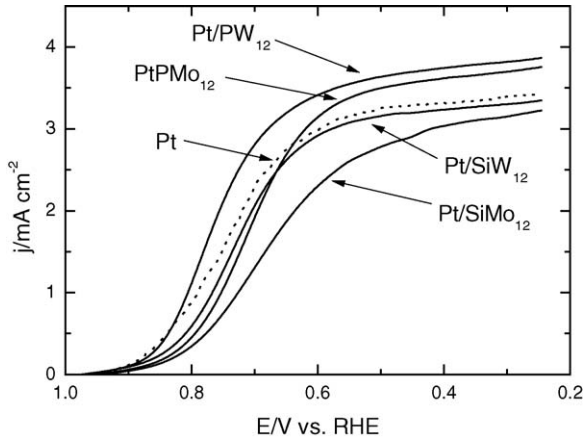

Fig. 4. RDE voltammograms recorded in the oxygen saturated 0.5 mol dm^{-3} H_2SO_4 using GC-supported Pt nanoparticles bare and modified with PW_{12}, PMo_{12}, SiW_{12}, or $SiMo_{12}$. Rotation rate, 1660 rpm. Scan rate, 5 mV s^{-1}.

surfaces were subsequently modified with POMs. The results of Fig. 4 imply that the highest current densities were obtained when GC-supported Pt nanoparticles were modified with PW_{12}. Also, from the viewpoint of stability (persistence of adsorption), the PW_{12} modified system seemed to be the most promising. Therefore, we concentrated on the latter system as the representative example of the Keggin type POM used for modification of the binary carbon-supported Pt electrocatalyst.

Fig. 5 shows the cyclic voltammetric response of the PW_{12}-modified GC-supported Pt nanoparticles recorded in the presence of oxygen. In the potential range down to 0 V, PW_{12} is characterized by the reversible one-electron process that can be described according to Eq. (1a). The related set of voltammetric peaks at about 0.25 V is overlapping the hydrogen adsorption peaks that typically exist at clean bare Pt (Fig. 3A). The system's (PW_{12}) second one-electron reduction reaction requires simultaneous injection of electron and proton [43] but its appearance on Pt is already complicated by the proton discharge reaction. Polytungstates adsorbed on Pt have been reported to interact with

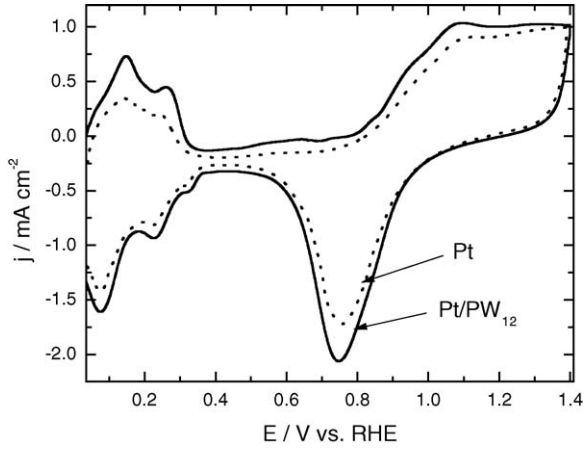

Fig. 5. Cyclic voltammetric response of PW_{12}-modified GC-supported Pt nanoparticles recorded in the oxygen saturated 0.5 mol dm^{-3} H_2SO_4. Scan rate, 50 mV s^{-1}. Dotted line illustrates the response recorded in the de-oxygenated solution.

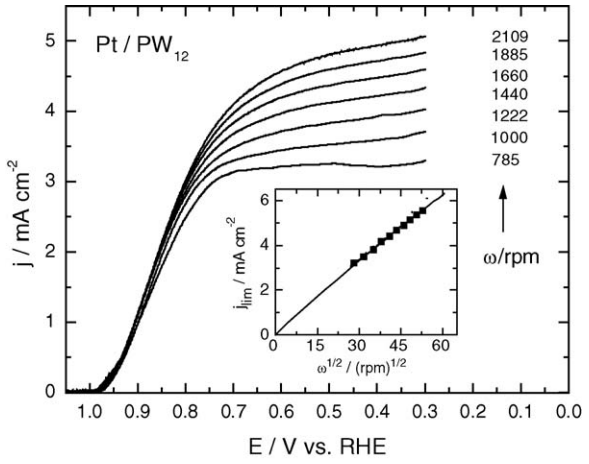

Fig. 6. RDE voltammograms recorded in the oxygen saturated ($C_{Ox} = 1.1 \times 10^{-6}$ mol cm^{-3} [48]) 0.5 mol dm^{-3} H_2SO_4 at different rotation rates using PW_{12}-modified GC-supported Pt nanoparticles. Scan rate, 5 mV s^{-1}. Inset shows the dependence of limiting current on the square root of rotation rate. Pt loading, 24 μg cm^{-2}.

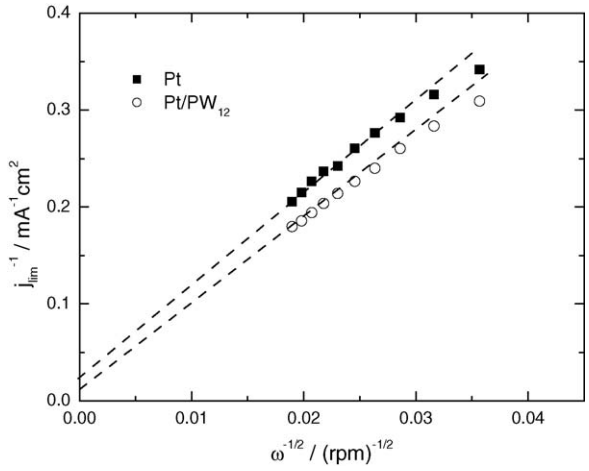

Fig. 7. Koutecky–Levich reciprocal plots prepared using the data of Fig. 6 for PW_{12}-modified GC-supported Pt nanoparticles. Currents were measured at 0.3 V. For comparison, the analogous plot is provided for bare (unmodified) GC-supported Pt nanoparticles of the same loading (24 μg cm^{-2}).

hydrogen adatoms to form mixed hydrogen/tungstate adlayers that are characterized by reversible redox behavior interpreted in terms of spillover effect [38]. The latter phenomenon explains fairly high reduction currents around 0.05–0.1 V, at least relative to what one would expect on bare (unmodified) Pt nanoparticles [39]. The appearance of the oxygen reduction peak at about 0.75 V is consistent with the view that the electrocatalytic reduction of oxygen proceeds at PW_{12}-modified Pt in a manner analogous to what has been observed at clean Pt [42] and bare Pt nanoparticles [39,43].

3.3. Diagnostic experiments with PW_{12}-modified carbon-supported Pt nanoparticles

To characterize further the PW_{12}-modified electrocatalyst, we have performed diagnostic RDE voltammetric experiments at different rotation rates (Fig. 6). The dependence of the respective RDE limiting currents versus the square root of rotation rate (inset to Fig. 6) shows some deviation from linearity (dotted line), i.e. from the ideal behavior characteristic of a system limited solely by convective diffusion of oxygen in solution, at rotation rates higher than ca. 1000 rpm. This result implies that only at faster rotation rates, the electrocatalytic reaction was too slow to allow the convective-diffusional control to be operative. Assuming the approximately first-order reaction kinetics [42], the RDE voltammetric limiting current densities (j_{lim}) can be described as reciprocals [36] using the Koutecky–Levich formalism

$$J_{lim}^{-1} = (nFk\Gamma_{film}C_{Ox})^{-1} + j_{Lev}^{-1} \quad (2)$$

where j_{Lev} limiting current density is given by the classic Levich equation (in which the convective diffusion component is proportional to the square root of rotation rate), k is a rate constant for the catalytic chemical reaction at the film/solution interface or within the film (in the homogeneous reaction meaning and units), Γ_{film} is the surface concentration of the catalytic centers in the film and C_{Ox} is the bulk concentration of oxygen in the electrolyte. The symbols n and F stand for the number of electrons involved in the process and the Faraday constant.

It is noteworthy that the Koutecky–Levich slopes in Fig. 7 are approximately the same for both PW_{12}-modified and bare GC-supported Pt nanoparticles. At potential as low as 0.3 V, platinum exists in its pure metallic form (i.e. where hydrogen adsorption peaks are absent and no platinum oxide is formed yet) and, in view of previous literature reports [42,44–47], it is reasonable to expect that $n = 4$ for bare platinum electrocatalysts. The similarity of slopes in Fig. 7 allows us to make the assumption about involvement of four electrons (implying the ideal reduction of oxygen effectively to water) in the case of PW_{12}-modified GC-supported Pt nanoparticles as well.

The analysis [36,42,44–46] of Koutecky–Levich reciprocal plots (Fig. 7) yielded for PW_{12}-modified GC-supported Pt nanoparticles a fairly small positive intercept equal to about 0.011 mA^{-1} cm^2. Using the approach described before [36], the kinetic parameter, namely the intrinsic rate constant of heterogeneous charge-transfer, k_{het} (which is equivalent to the product of $k\Gamma_{film}$ in Eq. (2)), has been found to be equal to ca. 2.2×10^{-1} cm s^{-1} for the catalytic electroreduction (in 0.5 mol dm^{-3} H_2SO_4) of oxygen at 0.3 V using the electrode of GC-supported Pt nanoparticles (loading, 24 μg cm^{-2}) modified with PW_{12}. When we have performed the analogous kinetic analysis for the electrode modified with PW_{12}-free Pt nanoparticles, the intrinsic rate constant is on the level 1×10^{-1} cm s^{-1}.

In the above considerations, it is provided that Koutecky–Levich lines are plotted (according to Eq. (2)) with the assumption of first-order reaction kinetics. Having in mind fast dynamics of charge transport in the catalytic film, the inverse proportionalities of the Koutecky–Levich slopes and intercepts with oxygen concentration (that have been found during the analysis of the RDE data obtained in the oxygen and air-saturated sulfuric acid solutions) support the above assumption. The unit reaction order was also reported in literatures [42,44,45] at different platinum based catalytic surfaces.

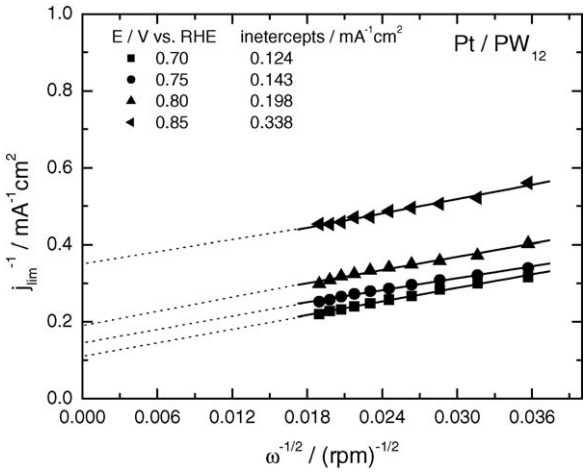

Fig. 8. Koutecky–Levich reciprocal plots prepared using the RDE currents of Fig. 6 measured at 0.7, 0.75, 0.80 and 0.85 V for PW_{12}-modified GC-supported Pt nanoparticles (loading, 24 μg cm^{-2}).

Fig. 8 shows Koutecky–Levich reciprocal plots recorded for the oxygen reduction at PW_{12}-modified GC-supported Pt nanoparticles using different potentials in the range from 0.70 to 0.85 V. The lines are almost parallel and the slopes are approximately identical. Since the number of electrons transferred (n in Eq. (2)) is a factor of the slope, we can conclude (from the parallelism of the lines in Fig. 8) that the reaction path for the oxygen reduction does not appreciably change with potential. Finally, the k_{het} heterogeneous reaction rate constants can be estimated at various potentials using the intercepts from Koutecky–Levich plots of Fig. 8. The values of k_{het} range from approximately 2×10^{-2} down to below 1×10^{-2} cm s^{-1} upon increasing the potential from 0.70 to 0.85 V. This decrease in k_{het} reflects presumably some inhibiting effect originating from platinum oxide formed on Pt at potentials higher than 0.6 V.

4. Conclusions

Modification of GC-supported platinum nanoparticles with PW_{12} has been demonstrated to produce highly reactive platinum centers towards reduction of oxygen. Like in the case of bare platinum, the overall reduction mechanism is unchanged and it seems to involve effectively four electrons producing directly water as a final product. It is apparent from kinetic analysis that formation of the ultra-thin monolayer-type PW_{12} films on Pt nanoparticles (and presumably GC substrate as well) exhibits some enhancement (synergistic) effect on the oxygen reduction. Having in mind the chemical analogies between PW_{12} and tungsten oxide, it is likely that the polyoxometallate provides similar environment to tungsten oxide/hydrogen bronzes [35,36]. The important issues are the ability of PW_{12} to form strong electroactive adsorbates on solid surfaces, its high reductive reactivity and fast electron transfer (mediating) capabilities, as well as its super-acid characteristics leading to the increased availability and mobility of interfacial protons. When combined with the specific reactivity of Pt inducing the reduction of oxygen, the above properties should promote a bifunctional electrocatalytic mechanism in which PW_{12} facilitates decomposition of the undesirable hydrogen peroxide intermediate. Judging from the data of Fig. 4, the promoting effect is restricted to PW_{12} and, to some extent, to PMo_{12} heteropolyacids. At this stage, it is unclear whether the slight inhibiting effect observed in the case of SiW_{12} and $SiMo_{12}$ originates from the lack of their profound chemical reactivity (towards H_2O_2 intermediate) or it comes from the possibility of passivation of Pt surface by adsorbed $SiMo_{12}O_{40}^{3-}$ or $SiW_{12}O_{40}^{4-}$ polyanions.

Acknowledgements

This work was supported by Ministero dell'Istruzione dell'Università e della Ricerca (MIUR), Italy, FISR 2001. The Warsaw group appreciates the partial support from Ministry of Science (Poland) under the State Committee for Scientific Research (KBN) grant 3 T09A 05426 and from the Network Efficient Oxygen Reduction for Electrochemical Energy Conversion (coordinated by ZSW, Ulm, Germany). R. W. and A. K acknowledge the University of Camerino for support.

References

[1] M. Sadakane, E. Steckham, Chem. Rev. 98 (1998) 219.
[2] D.E. Katsoulis, Chem. Rev. 98 (1998) 359.
[3] B. Keita, L. Nadjo, J. Electroanal. Chem. 243 (1988) 87.
[4] B. Keita, B.L. Nadjo, J.M. Saveant, J. Electroanal. Chem. 243 (1988) 105.
[5] O. Savadogo, J. Electrochem. Soc. 139 (1992) 1082.
[6] N. Giordano, A.S. Arico, S. Hocevar, P. Staiti, P.L. Antonucci, V. Antonucci, Electrochim. Acta 38 (1993) 1733.
[7] D. Martel, A. Kuhn, Electrochim. Acta 45 (2000) 1829.
[8] A. Papadakis, A. Souliotis, E. Papaconstantinou, J. Electroanal. Chem. 435 (1997) 17.
[9] N. Mizuno, M. Misono, Chem. Rev. 98 (1998) 199.
[10] I.V. Kozhevnikov, Chem. Rev. 98 (1998) 171.
[11] B. Keita, L. Nadjo, J. Haeussler, J. Electroanal. Chem. 243 (1988) 481.
[12] B. Wang, S. Dong, Electrochim. Acta 41 (1996) 895.
[13] S. Dong, Z. Jin, J. Chem. Soc. Chem. Commun. (1987) 1871.
[14] X. Xi, S. Dong, Electrochim. Acta 40 (1995) 2785.
[15] B. Keita, A. Belhouori, L. Nadjo, J. Electroanal. Chem. 314 (1991) 345.
[16] B. Keita, L. Nadjo, J. Electroanal. Chem. 240 (1988) 325.
[17] D. Ingersoll, P.J. Kulesza, L.R. Faulkner, J. Electrochem. Soc. 141 (1994) 140.
[18] S. Dong, W. Jim, J. Electroanal. Chem. 354 (1993) 87.
[19] K.K. Kasem, F.A. Schultz, Can. J. Chem. 73 (1995) 87.
[20] Y. Izumi, K. Urabe, Chem. Lett. (1991) 663.
[21] O. Nakamura, T. Kodama, I. Ogino, Y. Miyake, Japanese Patent JP 51,106,694 (1976);
O. Nakamura, T. Kodama, I. Ogino, Y. Miyake, Chem. Abstr. 86 (1976) 19085.
[22] O. Nakamura, T. Kodama, I. Ogino, Y. Miyake, US Patent 4,024,036 (1977).
[23] O. Nakamura, T. Kodama, I. Ogino, Y. Miyake, Japanese Patent JP 76,106,683 (1976);
O. Nakamura, T. Kodama, I. Ogino, Y. Miyake, Chem. Abstr. 86 (1976) 35749.
[24] N. Giordano, P. Staiti, S. Hecevar, A.S. Arico, Electrochim. Acta 41 (1996) 397.
[25] S. Hocevar, E. Passalacqua, M. Vivaldi, A. Patti, N. Giordano, Electrochim. Acta 41 (1996) 2817.
[26] M.W. Park, J.C. Yang, H.S. Han, Y.G. Shul, T.H. Lee, Y.I. Cho, Denki Kagaku, oyobi, Kogyo, Butsuri Kagaku 64 (1996) 743;
M.W. Park, J.C. Yang, H.S. Han, Y.G. Shul, T.H. Lee, Y.I. Cho, Chem. Abstr. 125 (1996) 15161.
[27] J.T. Kummar, D.-G. Oei, US Patent 4,396,687 (1983);
J.T. Kummar, D.-G. Oei, Chem. Abstr. 99 (1983) 161528.

[28] M. Akimoto, H. Niiyama, Japanese Patent JP 62,196,388 A2 (1987);
M. Akimoto, H. Niiyama, Chem. Abstr. 108 (1987) 13085.
[29] J.J. Kim, W.Y. Lee, I.K. Song, US Patent 5,227,141 A (1993);
J.J. Kim, W.Y. Lee, I.K. Song, Chem. Abstr. 120 (1993) 33373.
[30] R.F. Service, Science 305 (2004) 1225.
[31] M.W. Verbrugge, J. Electrochem. Soc. 141 (1992) 46.
[32] J.A. Poirier, G. Stoner, J. Electrochem. Soc. 141 (1994) 425.
[33] E.A. Ticianelli, C.R. Derouin, A. Redondo, S. Srinivasan, J. Electrochem. Soc. 185 (1988) 2209.
[34] O. Savadogo, K.C. Mandal, J. Electrochem. Soc. 139 (1992) L16.
[35] P.J. Kulesza, L.R. Faulkner, J. Electroanal. Chem. 259 (1989) 81.
[36] P.J. Kulesza, B. Grzybowska, M.A. Malik, M.T. Galkowski, J. Electrochem. Soc. 144 (1997) 1911.
[37] M. Chojak, M. Mascetti, R. Wlodarczyk, R. Marassi, K. Karnicka, K. Miecznikowski, P.J. Kulesza, J. Solid State Electrochem. 8 (2004) 854.
[38] M. Borzenko, M. Chojak, P.J. Kulesza, G.A. Tsirlina, O.A. Petrii, Electrochim. Acta 48 (2003) 3797.
[39] P.J. Kulesza, M. Chojak, K. Karnicka, K. Miecznikowski, B. Palys, A. Lewera, A. Wieckowski, Chem. Mater. 16 (2004) 4128.
[40] P.J. Kulesza, M. Skunik, B. Baranowska, K. Miecznikowski, M. Chojak, K. Karnicka, E. Frackowiak, F. Beguin, A. Kuhn, M.-H. Delville, B. Starobrzynska, A. Ernst, Electrochim. Acta, in press.
[41] A. Lewera, M. Chojak, K. Miecznikowski, P.J. Kulesza, Electroanalysis 17 (2005) 1471.
[42] S.K. Zacevic, J.S. Wainright, M.H. Litt, S.Lj. Gojkovic, R.F. Savinell, J. Electrochem. Soc. 144 (1997) 2973.
[43] P.J. Kulesza, K. Karnicka, K. Miecznikowski, M. Chojak, A. Kolary, P.J. Barczuk, G. Tsirlina, W. Czerwinski, Electrochim. Acta 50 (2005) 5155.
[44] N.M. Markovic, R.R. Adzic, C.D. Cahan, E.B. Yeager, J. Electroanal. Chem. 377 (1994) 24.
[45] D.B. Sepa, M.V. Vojnovic, Lj.M. Vracar, A. Damjanovic, Electrochim. Acta 32 (1987) 129.
[46] F. Maillard, M. Martin, F. Gloaguen, J.-M. Leger, Electrochim. Acta 47 (2002) 3431.
[47] J. Jiang, B. Yi, J. Electroanal. Chem. 577 (2005) 107.
[48] K.E. Gubbins, R.D. Walker, J. Electrochem. Soc. 112 (1965) 469.